URSI GASS 2023, Sapporo, Japan, 19 – 26 August 2023

Design of Series-Fed Antenna Array with Low SideLobe Level and Improved Azimuth Fied-of-View for Automotive RADAR Application

Jogesh Chandra Dash(1), Debdeep Sarkar(1), and Yahia M. M. Antar(2)
(1) Indian Institute of Science, Bangalore, India; e-mail: jcdash92@gmail.com, debdeep@iisc.ac.in
(2) Royal Military College of Canada, Kingston, ON, Canada; e-mail: antar-y@rmc.ca

Abstract

This paper proposes an eleven-element series-fed microstrip antenna array design with a low sidelobe level (SLL) using modified tapering and wide azimuth field-of-view (FoV) using parasitic array loading at 79 GHz for automotive short-range RADAR (SRR) application. Here, we highlight the design limitation of conventional series-fed antenna arrays with the binomial tapering approach to reduce the SLL at 79 GHz. The proposed modified tapering approach provides 25 dB of SLL, nearly 80^0 azimuth FoV, and 13.1 dBi peak gain. Further, the parasitic array loading in the close vicinity of the proposed tapered array yields 68.75% improvement in azimuth FoV i.e., 135^0 and 46.8% improvement in impedance bandwidth with 22 dB SLL.

1 Introduction

Modern vehicles are loaded with various technical services apart from conventional functions such as vehicle information and communication, the intelligent transportation system (ITS) for V2X connectivity, an advanced driver assistance system (ADAS), and many more [1], [2]. Among various services, ADAS is one of the important and crucial features because it provides active safety for the driver and the co-passengers. This ADAS system is supported by diverse sensor assemblies such as LiDAR, Camera, Ultrasonic, RADAR, and so on [3]. RADAR is considered a very robust and cost-effective sensor due to its immunity to weather and low-light conditions, and exhibits fewer integration challenges compared to optical sensors like LiDAR and cameras. Studies on automotive MIMO RADAR antenna integration challenges in a vehicle are provided in [4]-[7].

Automotive RADAR is classified into three groups such as long-range RADAR (LRR), medium-range RADAR (MRR), and short-range RADAR (SRR) to address appropriate distance and field-of-view (FoV) as shown in Table 1 [8], which provides 360^0 surveillance around the vehicle. LRR is a forward-looking RADAR that is normally used for adaptive cruise control (ACC) and MRR is generally used for medium-range applications such as cross-traffic alerts. However, the complete surrounding view of the vehicle is provided by SRR and therefore has special importance. SRRs are integrated at each corner of the vehicle and cater to applications such as blind spot detection, parking aid, and direct proximity sensing near the vehicle like obstacle detection. To accomplish these applications SRR requires antenna systems having wide azimuth FoV (see Table 1) for wide coverage and low sidelobe level to reduce false alarming.

Table 1. Automotive RADAR Classification.

Type	LRR	MRR	SRR
Azimuth FoV (3 dB beamwidth)	$\pm 15^0$	$\pm 40^0$	$\pm 80^0$
Elevation FoV (3 dB beamwidth)	$\pm 5^0$	$\pm 5^0$	$\pm 10^0$
Range (min.-max.)	$10-250$m	$1-100$m	$0.15-30$m

Among various antenna systems, a series-fed microstrip antenna array is one of the best possible choices for automotive RADAR applications to achieve low SLL and wide FoV. In addition, the lightweight and planar nature of the microstrip structure and edge feeding mechanism of series-fed array configuration provides an additional degree of freedom for easy integration to develop a complete RADAR module in a single platform. Achieving very low SLL for a series-fed array using the binomial tapering mechanism is one of the very conventional techniques [9], [10]. However, binomial tapering is not well conversant for an edge-feeding series-fed array configuration. To address this issue a seven-element series-fed array configuration using a modified binomial coefficient is proposed in [11], having SLL reduction below 16 dB. However, one of the key challenges in binomial tapering is to meet the fabrication challenges for a series-fed configuration having more than nine elements due to a very narrow width dimension for edge elements at the automotive SRR operating band ($77-81$ GHz). It is observed that the width of the edge elements is sometimes even less than its feed line width. Moreover, binomial tapering reduces the antenna gain.

There are different standard tapering mechanisms other than binomial one available in the open literature. In this paper, we highlight the tapering issue in an eleven-element series-fed binomial tapered antenna at 79 GHz SRR operating band and provide a new antenna design approach for eleven-element configuration thereby achieving SLL below 22 having a gain of 13.1 dBi. Moreover, we use parasitic series-fed array loading to improve the azimuth FoV

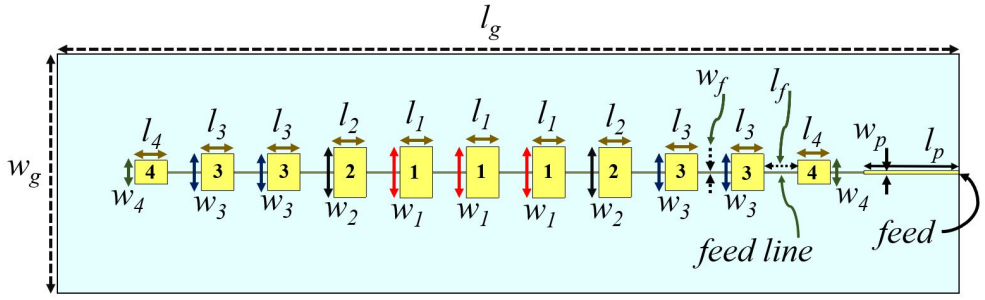

Figure 1. Schematic of the proposed eleven-element series-fed microstrip antenna array. Dimension in mm: $l_1 = l_2 = l_3 = l_4 = 1, w_1 = 1.6, w_2 = 1.56, w_3 = 1.15, w_4 = 0.74, l_f = 1.06, w_f = 0.045, l_p = 3, w_p = 0.1, l_g = 28.27, w_g = 7.55$.

to 135^0 from nearly 80^0 at a stand-alone antenna without parasitics.

2 Design Limitation of Binomial Tapering for Eleven-Element Series-Fed Array

Binomial tapering in an N-element (N = odd number, to provide design symmetry from the center element to the edge) series-fed array is incorporated in the width of each element of the array using the normalized binomial coefficient considering the center element as reference. The normalized coefficients of the binomial distribution for N-element can be written as

$$B_r = \frac{C_r^{N-1}}{C_{(N-1)/2}^{N-1}}, \tag{1}$$

where

$$C_r^{N-1} = \frac{(N-1)!}{r!.(N-1)!} \tag{2}$$

Here, C represents the mathematical symbol for combination and $r = 0, 1, ..., N-1$. The normalized binomial coefficients for the eleven-element series-fed array are as follows: where $r = 0, 1, ..., 10$.

$$B_r = \frac{C_0^{10}}{C_5^{10}}, \frac{C_1^{10}}{C_5^{10}}, \frac{C_2^{10}}{C_5^{10}}, \frac{C_3^{10}}{C_4^{10}}, \frac{C_4^{10}}{C_5^{10}}, \frac{C_5^{10}}{C_5^{10}}, \frac{C_6^{10}}{C_5^{10}}, \frac{C_7^{10}}{C_5^{10}}, \frac{C_8^{10}}{C_5^{10}}, \frac{C_9^{10}}{C_5^{10}}, \frac{C_{10}^{10}}{C_5^{10}} \tag{3}$$

$$= 0.003, 0.039, 0.179, 0.47, 0.66, 1, 0.66, 0.47, 0.179, 0.039, 0.003 \tag{4}$$

From (4), it is observed that the ratio between the edge element to its center element of an eleven-element series-fed array is 0.003. Translating this coefficient to the antenna design parameters, the width of the edge element is given by 0.004 mm at 79 GHz operating frequency (subject to the other design parameters such as 0.25 mm substrate thickness having $\varepsilon_r = 3$ and $\tan\delta = 0.001$), which signifies the design and implementation tolerance.

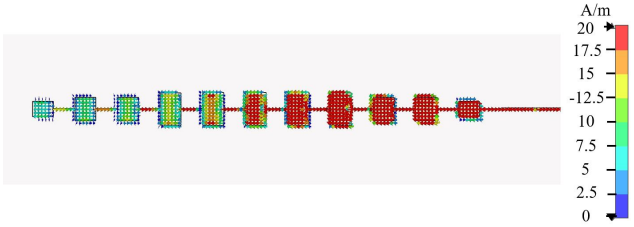

Figure 2. Vector surface current distribution at 79 GHz of antenna configuration shown in Fig. 1.

3 Design of Proposed Series-Fed Antenna Array

The schematic design of the proposed eleven-element series-fed antenna is shown in Fig. 1. The antenna is designed on a 0.25 mm thick substrate having $\varepsilon_r = 3$ and $\tan\delta = 0.001$ with an overall footprint of $l_g \times w_g = 28.27 \times 7.55$ mm^2. The other design parameters of the proposed antenna are provided in Fig. 1. Each array element has the same patch length of nearly $\lambda_g/2$ at the 79 GHz operating frequency. Since the microstrip antenna element provides 180^0 phase shift due to its resonating length, the connecting feed line length between the consecutive element is kept nearly $\lambda_g/2$ to provide an additional 180^0 phase shift for broadside radiation. The surface current distribution at 79 GHz frequency of the proposed antenna is shown in Fig. 2. In the proposed design a modified tapering approach is

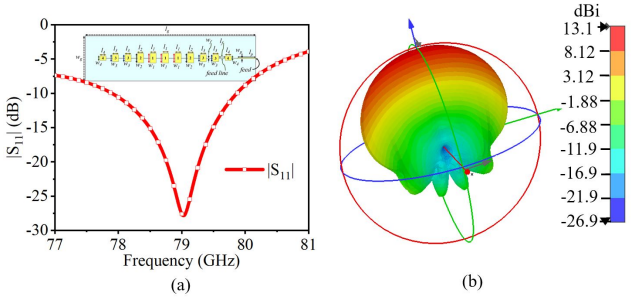

Figure 3. (a) Variation of S-parameter over frequency, and (b) 3D radiation pattern at 79 GHz showing gain of antenna configuration shown in Fig. 1.

adopted, unlike the conventional approach of tapering the consecutive element from the center to the edge of the array. In the proposed eleven-element array design the array elements are labeled as 1 to 4 (see Fig. 1) based on the decreasing order of their patch width, where array elements having the same label carry the same width dimensions. The proposed amplitude tapering approach by varying the patch width of the array elements gives rise to $w_1 = 1.6$ mm, $w_2 = 1.56$ mm, $w_3 = 1.15$ mm, $w_4 = 0.74$ mm (see Fig. 1). Further, the width of the feed line is adjusted to achieve the impedance matching at 79 GHz operating frequency. The S-parameter response of the proposed eleven-element series-fed tapered antenna resonating at 79 GHz having 1.974 GHz impedance bandwidth is shown in Fig. 3 (a). The antenna exhibits a peak gain of 13.1 dBi as shown in Fig. 3 (b). The proposed amplitude tapering exhibits an SLL reduction of 25 dB, the cross-pol level below 50 dB with elevation and azimuth FoV of 10^0 and $\approx 80^0$ respectively as shown in Fig. 4.

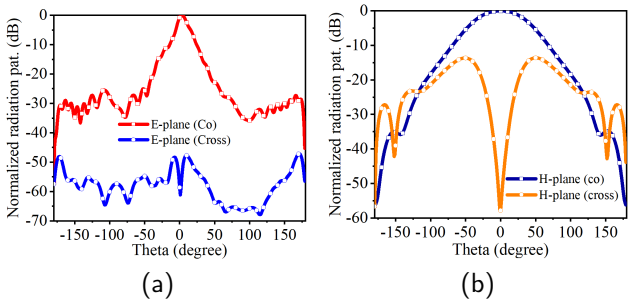

Figure 4. 2D radiation pattern of antenna array shown in Fig. 1 (a) E-plane, and (b) H-plane.

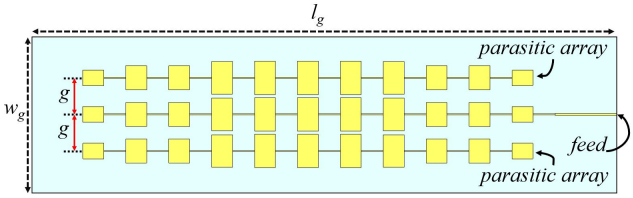

Figure 5. Schematic of parasitic array loaded eleven-element series-fed microstrip antenna array. Dimension in mm: $g = 1.75, l_g = 28.27, w_g = 7.55$.

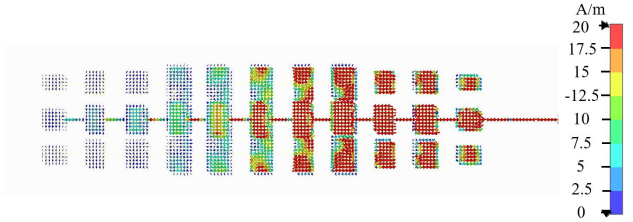

Figure 6. Vector surface current distribution at 79 GHz of antenna configuration shown in Fig. 5.

Further, to improve the azimuth FoV of the proposed antenna array (of Fig. 1) two additional parasitic arrays, identical to the primary radiator, are loaded in its vicinity as shown in Fig. 5. The surface current distribution at 79 GHz frequency of the parasitic array loaded antenna in Fig. 6 shows that due to the proximity coupling the surface current starts flowing in the parasitic array also, which improves the effective patch width. The parasitic array loading improves the antenna impedance bandwidth from 1.974 GHz to 2.898 GHz (46.8% improvement) due to an increase in the effective patch width without affecting the antenna operating frequency as shown in the S-parameter response of Fig. 7 (a). The peak gain of the parasitic array loaded antenna is 11.7 dBi as shown in Fig. 7 (b). The 2D radiation pattern of the antenna in Fig. 8 shows that the parasitic array loaded series-fed antenna exhibits an SLL reduction of nearly 22 dB with a wide azimuth FoV of 135^0, which is nearly 68.75% improvement compared to Fig. 1. A comparative study of various performance matrices between the antenna without and with parasitic loading is provided in Table 2 to provide better clarity.

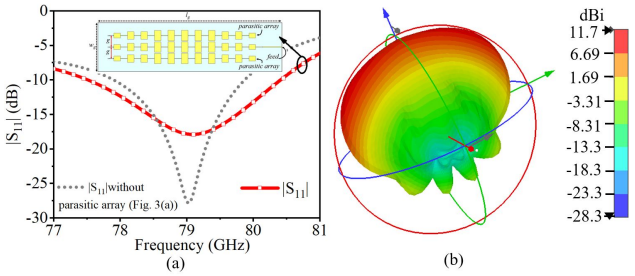

Figure 7. (a) Variation of S-parameter over frequency, and (b) 3D radiation pattern at 79 GHz showing gain of antenna configuration shown in Fig. 5.

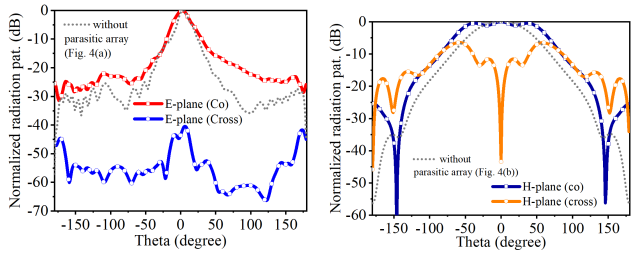

Figure 8. 2D radiation pattern of antenna array shown in Fig. 5 (a) E-plane, and (b) H-plane.

4 Conclusion

In this paper, we initially discussed the limitation of binomial tapering for an eleven-element microstrip series-fed

Table 2. Performance comparison between series-fed array (SFA) without and with parasitic loading.

Parameters	Series-Fed array without parasitic loading	Series-Fed array with parasitic loading
Operating frequency (GHz)	79	79
Impedance Bandwidth (GHz)	1.974	2.898
Azimuth FoV (3 dB beamwidth)	$\approx 80^0$	135^0
Elevation FoV (3 dB beamwidth)	14.2	20.7
Peak Gain (dBi)	13.1	11.7
Side-lobe level (dB)	25	22

array at 79 GHz. Further, we propose a modified tapering approach for an eleven-element series-fed array at 79 GHz operating frequency, thereby achieving an SLL reduction of 25 dB with $\approx 80^0$ azimuth FoV. Thereafter, we extend the proposed series-fed array design to increase azimuth FoV using parasitic array loading, thereby achieving 68.75% azimuth FoV improvement to 135^0. In addition, it provides a 46.8% improvement in impedance bandwidth with an SLL reduction of 22 dB. The proposed series-fed antenna design with improved azimuth FoV and bandwidth is suitable for automotive SRR applications.

Acknowledgements

The work is jointly supported by the Institute of Eminence (IoE)-IISc Post-Doctoral Fellowship and Society for Innovation and Development (SID)-IISc, DoT, GoI.

References

[1] C. Waldschmidt, J. Hasch and W. Menzel, "Automotive radar - from first efforts to future systems," *IEEE Microw. Mag.*, vol. 1, no. 1, pp. 135-148, Jan. 2021.

[2] V. K. Kukkala, J. Tunnell, S. Pasricha and T. Bradley, "Advanced driver assistance systems: a path toward autonomous vehicles," *IEEE Consum. Electron. Mag.*, vol. 7, no. 5, pp. 18-25, Sept. 2018.

[3] E. Marti, M. A. de Miguel, F. Garcia and J. Perez, "A Review of Sensor Technologies for Perception in Automated Driving," in *IEEE Intelligent Transportation Systems Magazine*, vol. 11, no. 4, pp. 94-108, winter 2019.

[4] J. C. Dash and D. Sarkar, "Antennas for mm-wave MIMO RADAR", in *Handbook of Metrology and Applications*, D.K. Aswal, et.al, Springer, Singapore, 2023. https://doi.org/10.1007/978-981-19-1550-5_82-1.

[5] J. C. Dash and D. Sarkar, "Antenna Array Ambiguity Function Based Study of Integration Effect on a 2D Automotive MIMO RADAR Antenna Placed Behind a Painted Bumper ", *2022 URSI Regional Conference on Radio Science (RCRS)*, 2022.

[6] J. C. Dash and D. Sarkar, "Impacts on Automotive MIMO RADAR Performance due to Permittivity Variation of Bumper Material: Insights through Bidirectional Loss and Antenna Array Ambiguity Function", *2021 IEEE MTT-S International Microwave and RF Conference (IMARC)*, 2021, pp. 1-4.

[7] J. C. Dash et al., "Performance Evaluation of Automotive RADAR in The Presence of Bumper with Multiple Paint Layers Using Bidirectional Loss Model," *2021 15th European Conference on Antennas and Propagation (EuCAP)*, 2021, pp. 1-5.

[8] J. Hasch, E. Topak, R. Schnabel, T. Zwick, R. Weigel, and C. Waldschmidt, "Millimeter-wave technology for automotive radar sensors in the 77 GHz frequency band," *IEEE Trans. Microw. Theory Techn.*, vol. 60, no. 3, pp. 845–860, Mar. 2012.

[9] C. A. Balanis, *Antenna Theory: Analysis and Design*. Hoboken, NJ: Wiley, 2016.

[10] R. Chopra and G. Kumar, "Series-Fed Binomial Microstrip Arrays for Extremely Low Sidelobe Level," *IEEE Trans. Antennas Propag.*, vol. 67, no. 6, pp. 4275-4279, June 2019.

[11] J. C. Dash, D. Darkar and Y. Antar, "Design of Series-fed Patch Array with Modified Binomial Coefficients for MIMO RADAR Application," *2021 IEEE AP-S Symposium on Antennas and Propagation and USNC-URSI Radio Science Meeting*, 2021.